Monte Carlo simulations of finite-size effects in Kosterlitz Thouless systems

1989 J. Phys.: Condens. Matter 1 5139

(http://iopscience.iop.org/0953-8984/1/31/012)

J. Phys.: Condens. Matter 1 (1989) 5139–5150. Printed in the UK

Monte Carlo simulations of finite-size effects in Kosterlitz–Thouless systems

F Falo†, L M Floría‡ and R Navarro†

† Departamento de Ciencia y Tecnología de Materiales y Fluídos, Instituto de Ciencia de Materiales de Aragón, Universidad de Zaragoza—CSIC, 50015 Zaragoza, Spain

‡ Departamento de Matemática Aplicada, Instituto de Ciencia de Materiales de Aragón, Universidad de Zaragoza—CSIC, 50015 Zaragoza, Spain

Received 22 July 1988, in final form 28 January 1989

Abstract. The two-dimensional planar rotator and XY ferromagnetic models for finite lattice sizes (triangular network), with free and periodic boundary conditions, have been studied using Monte Carlo simulations. Thermodynamic quantities, suitable for comparison with experimental data, have been obtained. Heat capacity data are almost insensitive to the lattice size and to the type of boundary conditions, whereas susceptibility data are sensitive to both the lattice size and the boundary conditions. For the Kosterlitz–Thouless phase transition non-universal critical parameters are inferred. They depend on the lattice, the model and the boundary conditions. It is conjectured that the main differences between free and periodic boundary conditions are caused by the influence of the free surface on vortex energetics.

1. Introduction

Since Kosterlitz–Thouless (KT) (Kosterlitz and Thouless 1973, Kosterlitz 1974) explained the contradictory theoretical results for two dimensional (2D) magnetic systems, in which the susceptibility (χ) has a divergence with zero magnetisation (M), a great effort on both theoretical and experimental aspects has been made. 2D planar magnetic models are examples of systems with linear and non-linear excitations, extended spin waves and localised vortices. At low temperatures spin waves dominate and long-range order is destroyed ($M = 0$), but short-range order (SRO) still exists and it is characterised by a power-law decrease of the correlation function, which yields infinite susceptibility. The transition to a disordered phase is caused by non-linear and localised vortex-like excitations, which at low temperatures appear in bounded couples and at higher temperatures dissociate thereby destroying the SRO.

Conventional perturbative methods enable an accurate spin-waves treatment to be undertaken. However, due to their intrinsic non-linear nature, the vortices cannot be handled in the same way and non-perturbative methods, such as renormalisation group (RG) (José *et al* 1977) or Monte Carlo (MC) simulations (Tobochnik and Chester 1979) have proved to be powerful tools in calculating the effects of vortices. In particular, a cusp in the specific heat, at temperatures for which χ is finite, has been detected using MC simulations. The correlation function, the vortice density and other macroscopic quantities have also been estimated. Most of the MC calculations have been carried out

0953-8984/89/315139 + 12 $02.50

for the square lattice planar rotator (PR) and XY models and, if bulk properties are to be simulated, periodic boundary conditions (PBC) must be included (Tobochnik and Chester 1979, Landau and Binder 1981, Gerling and Landau 1984). However, as far as we know, no such MC studies have been made on these models for finite-size lattices, in which neither the thermodynamic limit nor PBC may be applied. Free boundary conditions (FBC) imposed on finite clusters could drastically change the vortice-creation mechanism and could also modify the non-universal parameters of the phase transition. Thus, for half-infinite systems it has been shown that, because of the appearance of image vortices, single vortices pass over the boundary (Holz and Gong 1987).

From an analytical point of view, finite-size effects have been studied by Szeto and Dresselhaus (1985), who used RG methods to interpolate the low-temperature spin-wave and the high-temperature regimes. Their RG method, although correct, is unable to take into account two main features: (1) spin-wave–vortex interaction, since the RG method uses Villain's approximation, which is known to fail in the quantitative description of the KT phase transition (Janke and Kleinert 1986); and (2) non-periodic boundary conditions, because the RG method uses the spin-wave approximation, in which PBC are required, since the Brillouin zone must be well defined.

On the experimental side, many systems (not only of a magnetic nature) have confirmed some of the theoretical predictions. Superfluidity in two dimensions, 2D melting, and the adsorption of gases onto crystalline surfaces are examples to which the KT theory of 2D-phase transitions has been applied (Sinha 1980). In spite of the fact that the KT theory was initially developed for 2D-spin systems, its direct application to magnetic systems has been very rare and difficult to use in comparison. Magnetic layered systems like $Rb_2Cr\,Cl_4$ or $BaM_2(XO_4)_2$ compounds (M = Co, Ni and X = P, As) present a phenomenology understood as planar and 2D (Regnault *et al* 1984). Though these compounds have a ratio $J'/J \simeq 10^{-3}$, 10^{-4} between inter- (J') and intra- (J)) layer exchange interaction constants, the KT transition is masked by the crossover to three dimensional (3D) behaviour. This crossover, so far studied for Ising and Heisenberg models with high temperature series expansion (HTS) (Puértolas *et al* 1985) and with MC simulations (Kawabata and Bishop 1986), must dominate at a sufficiently low temperature and may forbid the KT phase transition.

Better candidates to exhibit 2D-magnetic behaviour seem to be the graphite intercalated compounds (GIC) with magnetic ions. In particular, the 2D character of the GIC of Cl_2Co or Cl_3Fe, along with the fact that crystal field effects reduce the spin dimensionality to $D = 2$, suggests that KT transitions may be observed experimentally in these systems (Dresselhaus 1986). Moreover, for any fit of the experimental results to the theoretical predictions, one should realise that these intercalated compounds form clusters, mainly due to the synthesis procedure. Therefore, the possible lack of correlation between different clusters makes the study of planar magnetic models on finite-size systems, with arbitrary boundary conditions, sensible.

For this purpose, MC simulations are most adequate, since not only are any kind of boundary conditions easily implemented, but the non-linear character of the vortex–antivortex excitation and spin-wave–vortex interaction is also dealt with straightforward. With this aim, MC simulations on both 2D-PR and XY models

$$H_{PR} = -JS^2 \sum_{\langle i,j \rangle} \cos(\varphi_i - \varphi_j) \qquad \text{(PR model)} \qquad (1a)$$

$$H_{XY} = -JS^2 \sum_{\langle i,j \rangle} \sin\theta_i \sin\theta_j \cos(\varphi_i - \varphi_j) \qquad (XY \text{ model}) \qquad (1b)$$

have been performed. In the above expressions θ_i and φ_i are the polar and azimuthal angles of the spin at site 'i', respectively, referred to an arbitrary direction, and the summation is restricted to nearest neighbours. The first Hamiltonian, H_{PR}, is used to analyse a 2D system of two-dimensional ($D = 2$) classical spins and this is considered with the second one, H_{XY}, a 2D net of three dimensional ($D = 3$) classical spins, in which only the planar components interact. In both models the spin length is normalised to $S^2 = 1$.

Boundary conditions have been chosen to be either free or periodic, as defined in the usual way. Moreover, a planar triangular (PT) lattice has been chosen to obtain non-universal parameters for the KT transition and to compare the results with the experimental ones on Cl_2Co-GIC, which has been the subject of a previous communication (Falo and Navarro 1988).

The present contribution, therefore, is mainly devoted to the analysis, through MC simulations, of clusters in planar 2D models. First, a brief description of the MC algorithms used is given and, furthermore, to check these methods bulk behaviour comparisons with spin-wave theory and HTS results are presented. Secondly, calculations for both models and for different lattice sizes and boundary conditions are also performed. Finally, the main parameters of the transitions have been determined and the results have been analysed and discussed in the light of the KT theory.

2. Monte Carlo algorithms

Monte Carlo simulations have been performed using a conventional Metropolis algorithm and, to assure better statistics in the results and to save computing time, some modifications have been implemented. First, to obtain an acceptance ratio above 0.5, a maximum range of spin variation is allowed and sweeping the lattice sequentially, each Monte Carlo step (MCS) is obtained. A random number, r_1, in the interval $[-0.5, 0.5]$ is chosen and the angle φ_i changed to $(1 + \omega r_1)\varphi_i$ in the PR model, whereas, in the XY case, S_i^z becomes $(1 + \omega r_1)S_i^z$ ($\omega < 1$ is self-consistently chosen to get an acceptance ratio of 0.5). The energy of the new configuration is calculated and the change accepted if the difference from the previous one, ΔE, is lower than zero or if $e^{-\Delta E/T} > r_2$ (r_2 being another random number in the interval $[0, 1]$ and T, the reduced temperature of the system). In our case, the change has been tried three times on the same site. This method (Diep *et al* 1985) speeds up the convergence to equilibrium and decreases the statistical correlations length between spin configurations. Note that with this method each MCS used here is equivalent to several usual MCS.

To enable the system to reach thermal equilibrium, over 5×10^3 MCS were discarded. Then, thermodynamic functions were obtained by averaging over some thousands (about 10^4) MCS. For each lattice size several MC simulations, either lowering the temperature or increasing it, were performed. In the process, the initial configuration for each temperature was the last one derived in the previous simulation. Moreover, though different initial spin configurations were used, the same results were always obtained.

The thermodynamic quantities obtained from the MC simulations are as follows.

(i) The order parameter, defined as the absolute value of magnetisation m_L,

$$m_L = \left(\sum_i \cos\varphi_i, \sum_i \sin\varphi_i\right)/N \qquad \text{(for the PR model)} \tag{2}$$

$$m_L = \left(\sum_i \sin\theta_i \cos\varphi_i, \sum_i \sin\theta_i \sin\varphi_i\right)/N \qquad \text{(for the } XY \text{ model)} \tag{3}$$

L being the lattice linear dimension and $N = L \times L$ the number of spins.

(ii) The specific heat per spin and the reduced susceptibility,

$$C_v = (\langle E^2\rangle - \langle E\rangle^2)/(k_B T)^2 \tag{4}$$

$$\chi_L = N(\langle m_L^2\rangle - \langle |m_L|\rangle^2) \tag{5}$$

where E is the internal energy per spin and k_B the Boltzmann constant. It is well known that $\langle m_L\rangle = 0$ for the infinite lattice ($L \to \infty$) and, therefore, it is convenient to define

$$\chi_\infty = N\langle m_L^2\rangle \tag{6}$$

$\chi_\infty = \chi_{exp} T/C$, C being the Curie constant.

(iii) The vorticity and the vortex density have also been considered. The vorticity, m_i, is usually defined as

$$m_i = (1/2\pi)\sum_{\Delta} (\varphi_i - \varphi_j) \tag{7}$$

where the summation extends over each plaquette in the lattice (triangular in our case). The vortex density is defined as

$$\rho_v = (1/N)\sum_i (m_i)^2. \tag{8}$$

Statistical errors were estimated using 'coarse graining' averages and carrying out correlation time, τ_c, calculations. In all cases τ_c was found to be much smaller than the number of MCS used in the simulations, even near the critical point, where an important increase in τ_c is expected (critical slowing down).

3. Check of MC simulations

It is worthwhile to compare the MC results with those obtained by other techniques, to check simulation programs and procedures. Moreover, this comparison also enables the validity range of the approximations as well as the extent of finite-size effects to be estimated. In the low-temperature regime, where the validity of the spin-wave theory (SWT) is well proven, this comparison has already been used by Tobochnik and Chester (1979) to test their earlier MC simulations. For the PT lattice and PR model the magnetisation and heat capacity, in the simplest SWT, are given by

$$\langle |m_L|\rangle = N^{-\Delta} \tag{9}$$

where $\Delta = T/6\pi J$

$$C_v = k_B/2. \tag{10}$$

Unfortunately, SWT is valid only for very low temperatures ($T/J < 0.3$), but a simple approximation by Samuel (1982), which hereafter will be called self-consistent spin-wave theory (SCSWT), allows the validity of the SWT results to be extended to higher

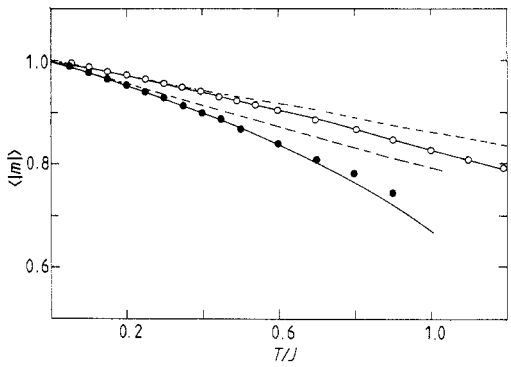

Figure 1. Comparison of the absolute values of the magnetisation obtained for the PR (open symbols) and XY (full symbols) models by: MC simulations on a 16×16 spin lattice with PBC (circles); SWT (dashed curve) and SCSWT (continuous curve).

temperatures. If a Hartree-Fock approximation for the PR Hamiltonian (1) is used, an effective Hamiltonian, H_{eff}, can be obtained, namely

$$H_{\text{eff}} = \frac{J}{T}\sum_{\langle ij\rangle}\frac{(\varphi_i - \varphi_j)^2}{2}\exp[-\langle(\varphi_i - \varphi_j)^2\rangle/2]. \tag{11}$$

From (11), $\langle(\varphi_i - \varphi_j)^2\rangle/2 = \Phi$ is derived as the solution of the self-consistent equation

$$\Phi = \frac{T}{J}e^{\Phi}(G(0) - G(\delta)) = \frac{T}{J}e^{\Phi}\int_{\text{BZ}} dk\,\frac{1 - \exp(i\boldsymbol{k}\cdot\boldsymbol{\delta})}{z - z\gamma_k} \tag{12}$$

where $\boldsymbol{\delta}$ is a vector that joins next-nearest neighbours, z the lattice coordination number, $\gamma_k = (1/z)\Sigma_\delta e^{i\boldsymbol{k}\cdot\boldsymbol{\delta}}$ and the integration extends over the first Brillouin zone (BZ). $G(0) - G(\delta)$ is $\frac{1}{4}$ for the square lattice and $\frac{1}{6}$ for the PT one. Equation (12) enables an effective temperature, $T_{\text{eff}} = Te^{\Phi}$, to be defined that, substituted in (9), gives a new dependence for the magnetisation. A similar procedure can be implemented for the XY model and for this case two self-consistent equations are obtained

$$\alpha = (T/12J)\,e^{\alpha}/(1 - e^{-\Psi_0}\,\Psi_0)(1 - e^{-\alpha}\alpha) \tag{13a}$$

$$\Psi_0 = (T/6J)\,e^{\Psi_0}\,1/(1 - e^{-\alpha}\,\alpha) \tag{13b}$$

where $\alpha = \langle\Phi_i^2\rangle/2$, $\Phi_i = ((\pi/2) - \theta_i)$ and $\Psi_0 = \langle(\varphi_i - \varphi_j)^2\rangle/2$.

In figure 1, comparisons of the magnetisation calculated using MC simulations for a 16×16 spin lattice with PBC, as well as the results using SWT and SCSWT, are shown for the PR (open symbols) and XY (full symbols) models. The agreement with SCSWT predictions (continuous curve) is excellent up to $0.8T_c$ (T_c is critical temperature). For higher temperatures there are systematic deviations, probably due to the appearance of an increasing number of vortices, a fact that a perturbative theory is unable to take into account.

In the high temperature limit, exact HTS expansions have shown to be a powerful tool in the study of phase-transitions phenomena, even up to the critical region (Domb and Green 1974). Eleven and 12 HTS coefficients for C_v and χ, respectively, are known for the PT lattice (Ferer and Velgakis 1983, Ferer *et al* 1984), from which a direct computation of such quantities is possible. Moreover, to enlarge the convergency radius of the C_v and χ HTS, direct Padé approximants (PA) have been used to extrapolate the

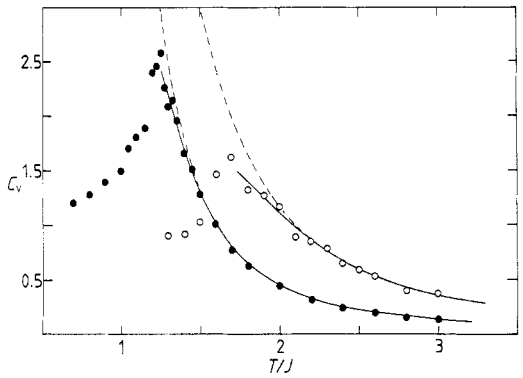

Figure 2. Comparison of the specific heat per spin derived for the PR (open circles) and XY (full circles) models from: MC simulations on a 30×30 spin lattice with PBC (circles); direct evaluation of HTS (dashed curve) and PA extrapolations (full curve).

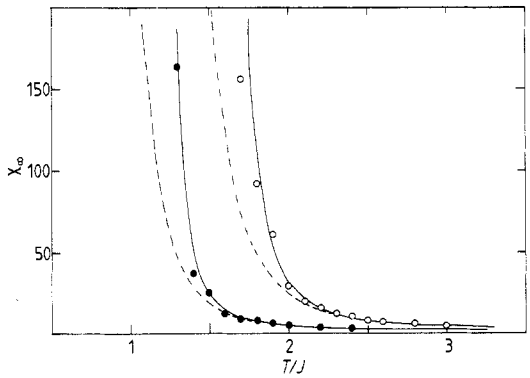

Figure 3. Comparison of the reduced susceptibility calculated for the PR (open symbols) and XY (full symbols) models by means of: MC simulations on a 30×30 spin lattice with PBC (circles); direct evaluation of HTS (dashed curve) and PA extrapolations (continuous curve).

results to a wider temperature range. In figures 2 and 3 the results obtained for the PR and XY models from direct HTS (dashed curves) and by means of PA (continuous curve) calculations are compared with the MC simulations for PBC on a 30×30 spin lattice, which is supposed to be large enough to mimic the bulk behaviour. The MC results for C_v (circles of figure 2) fit fairly well the PA ones, almost up to the cusp. However, the series has a bad convergency and the cusp, when placed at a temperature, T_p, higher than T_c, cannot be obtained from the HTS coefficients actually known. Moreover, there is a difference between direct HTS results and PA extrapolations, which proves the failing of the former.

In the same temperature limit and for the case of χ, results derived by the same procedures are plotted in figure 3. The χ values computed from the HTS deviate from both PA and MC estimations at about $1.6T_c$. Moreover, systematic differences appear between the PA and MC results for temperatures near T_c (about $1.3T_c$), which are due to finite-size effects of the lattice used, because other MC simulations with different lattice sizes yield results that do not coincide at such temperatures, as will be seen in the next section.

4. Results

4.1. Planar rotator model

Simulations on the 2D PR model with PBC were performed for four different lattice sizes ($L \times L$, $L = 12, 24, 30$ and 48). The results for the energy and susceptibility are shown

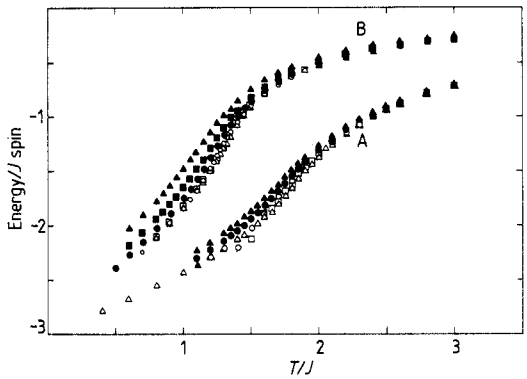

Figure 4. Internal energy in dimensionless units, as a function of temperature, for the PR (A) and XY (B) models and for different spin-lattice sizes. Open symbols correspond to PBC and full ones to FBC. Triangles (12 × 12), squares (24 × 24), and circles (48 × 48).

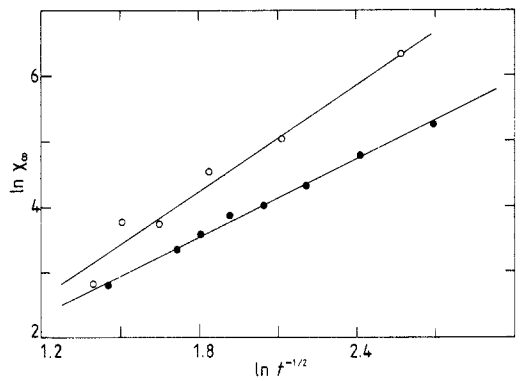

Figure 5. Double logarithmic representation of the χ MC simulation results for the PR model with PBC (open symbols) and FBC (full symbols) for a 60 × 60 spin lattice. The continuous curve corresponds to the best fit to expression (14), with the critical parameters given in the text.

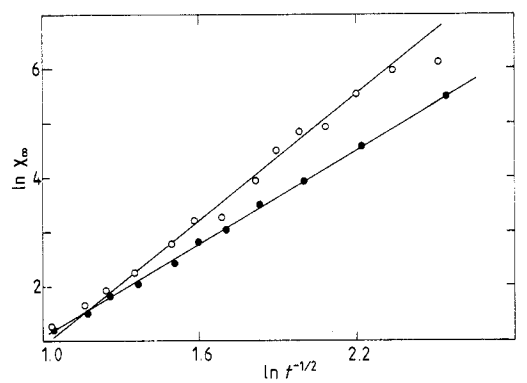

Figure 6. Double-logarithmic representation of the χ MC simulation results for the XY model with PBC (open symbols) and FBC (full symbols) for a 60 × 60 spin lattice. The lines have the same meaning as for figure 5.

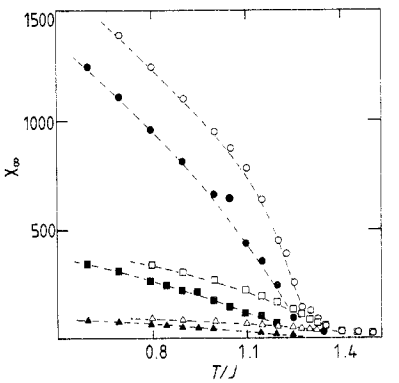

Figure 7. Reduced susceptibility derived by means of MC simulation for the XY model with PBC (open symbols) and FBC (full symbols) for different spin-lattice sizes. The dashed curves are guides to the eye. Symbols are the same as for figure 4.

in figures 4 to 7. A very small dependence of the energy data on the lattice size is observed (see figure 4). The heat-capacity curve shows a sharp cusp which rapidly saturates with increasing size. The cusp occurs at $T_p/J \simeq 1.75$, which is higher than the corresponding one for the square lattice (Tobochnik and Chester 1979).

Although T_c is not well defined in finite systems (Barber 1983), a rough estimation may be obtained if the critical behaviour of the reduced susceptibility for infinite KT systems is used, namely

$$\chi = A \exp(bt^{-1/2}) \qquad \text{with} \qquad t = (T - T_c)/T_c \tag{14}$$

where b and T_c are non-universal lattice and model-dependent parameters and will even also depend on boundary conditions. When the correlation length for a particular temperature is larger than the dimension L, the results of the simulation, which cannot become infinite, will deviate from those derived with expression (14). In spite of this fact, there is a wide temperature range in which an exponential variation is followed (see figure 5) and it is interesting to calculate these parameters from data obtained using finite lattice sizes. To avoid troubles due to finite size, in each simulation the largest possible lattice that will enable points near the transition to be less influenced by finite size has been used. For PBC, (open circles of figure 5) the best fit of the simulation to expression (14) yields $T_c/J = 1.39 \pm 0.02$ and $b = 2.7$. This T_c value is in agreement with the one previously reported (Ferer and Velgakis 1983) determined using a four-fit analysis of χ HTS.

The same simulations with FBC on the PR model for $L \times L$ ($L = 30, 60$) spin lattices show an appreciable dependence of the energy with the lattice size (figure 4, full symbols). The results almost overlap at higher temperatures with those for PBC and as temperature decreases their differences increase. One of the reasons for such behaviour may be found in the contribution to the energy of the surface spins, since some neighbours are missing in the lattice edges. For larger sizes the energy values converge on the PBC results, though more slowly than expected if the decrease of the relative number of spins at the surface is considered. In the case of FBC no saturation was found for the C_v cusp, although minor differences in both height and position are observed.

For the largest spin lattice (60×60) the results for the χ MC simulations have been plotted in figure 5 and fitted to expression (14). The critical parameters derived $T_c/J = 1.5 \pm 0.05$ and $b = 2.05$, show small differences for T_c from the value obtained using PBC, but the parameter b is unambiguously lower.

4.2. *XY model*

For the analysis of the XY model with PBC, MC simulations on $L \times L$ spin lattices ($L = 12, 24, 30, 48$) have been used. The energy versus temperature results are shown in figure 4 (open symbols). Their behaviour is similar to that for the PR model and again a cusp in C_v is observed, but at lower temperature, $T_p/J = 1.30$. This lower T_p is related to the smaller energy required for the creation of a vortex–antivortex pair, since in the XY model the classical spins may have a non-zero z-component.

A similar analysis performed on a 48×48 spin lattice yields the χ MC simulation results shown in figure 6 for PBC. The best fit to expression (14) was obtained for $b = 3.8$ and $T_c/J = 1.03 \pm 0.02$, which are values in agreement with HTS results (Ferer and Velgakis 1983).

The same systematic simulations have been performed for the XY model with FBC and in figure 4 the internal energy as a function of the temperature is shown. Again, great changes due to the lattice-size effects are observed and furthermore this influence is also observed in C_v, although the differences up to T_p are minor.

As for the PR model, there is an appreciable quantitative difference between the MC χ simulation results for the same spin-lattice size depending on the boundary conditions,

which affects the critical parameters. The best fit to expression (14) yields $T_c/J = 1.04 \pm 0.02$ and $b = 2.8$ (see figure 6). While this T_c coincides with the T_c (PBC), the b value shows a large difference with respect to b(PBC), which reflects the different magnitude of χ.

5. Discussion

A first non-trivial conclusion of the above results, which may help the experimentalist dealing with GIC-type compounds, is the near insensitivity of C_v to finite-size effects. For PBC there is no dependence of the internal energy per spin on the finite-size spin lattice, whereas for FBC, although the energy depends on the spin-lattice size, there are minor variations in the bulk quantity C_v. Contrarily, χ is very sensitive to both size and boundary conditions.

On the other hand, the results show some expected and well known features, as follows. First, the T_p and T_c values for the PT lattices reported here are different from those published (Tobochnik and Chester 1979) for the square one, and also the ratio T_p/T_c(PT) also differs from T_p/T_c(square). These differences were expected, since neither T_p nor T_c are universal critical parameters. Savit (1980) has predicted a relationship between the critical temperatures for both lattices, $T_c(\text{PT}) \approx 3^{1/2} T_c(\text{square})$, which is roughly fulfilled by the results obtained here. However, the relative difference between T_c and T_p for the square lattice is about 10%, whereas for the PT one the relative difference amounts to 25–30%.

The qualitative differences between relevant quantities obtained by MC simulations for the PR and XY models in the PT lattice are similar to those obtained for the square lattice, as expected. The possibility of tilting the spins up for the XY model decreases the spin projection on the xy-plane, which lowers the transition temperatures. Then, the energy needed to create a vortex–antivortex pair in XY model is expected to be lower than in the PR one.

In figure 7 the temperature-dependence of χ_∞ for the XY model with both PBC and FBC and different lattice sizes is shown. From inspection of this figure one concludes that the finite-size effects strongly depend on the boundary conditions, which is also observed in the PR model. It should be noted that b-values for FBC are always smaller than those for PBC. These results indicate that, depending on the boundary conditions, it seems that different mechanisms govern the phenomenology near T_c. This may be studied by analysing the vortex–antivortex pair creation energy, E_v, for both models.

To this end expressions (7) and (8) for the vorticity and vortex density, respectively, have been calculated using MC simulations with both types of boundaries. If a temperature-dependence of the vortex density of the form

$$\rho_v(T) \approx \exp(-E_v/k_B T) \tag{15}$$

is assumed, a mean value E_v may be determined from a least-squares $\rho_v(T)$ against T fit. This relationship has been found to be reasonably well fulfilled in a wide temperature range, both for FBC and for PBC, even well below T_c. In table 1 the E_v values obtained for the PR and XY models are summarised. For PBC, a 30×30 spin lattice, as being representative of the bulk behaviour, has been used, because for PBC an energy variation with the lattice size is not expected. The vorticity has a great influence on the specific heat (Ami and Kleinert 1982) and for PBC it saturates rapidly with increasing lattice size.

Table 1. Mean vortex–antivortex creation energy in normalised dimensionless units E_v/zJ (z = number of next neighbours) for the PR and XY models applied to the PT lattice, for different boundary conditions and different spin-lattice sizes. For comparisons the results for the square net (Gerling and Landau 1984, Landau and Binder 1981) are included.

Model	PBC (30 × 30)	FBC (30 × 30)	FBC (60 × 60)	Square-lattice PBC
PR	2.20 ± 0.03	1.70 ± 0.03	1.82 ± 0.03	2.45
XY	1.67 ± 0.03	1.39 ± 0.02	1.42 ± 0.03	1.58

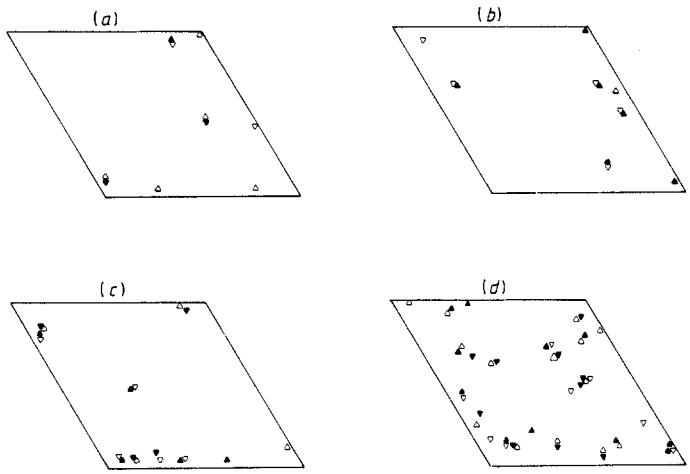

Figure 8. Typical vortices (open symbols) and antivortices (full symbols) configurations for the PR model with FBC at different reduced temperatures: (*a*) $T/J = 1.30$; (*b*) $T/J = 1.40$; (*c*) $T/J = 1.45$; (*d*) $T/J = 1.50$; ($T_c/J \simeq 1.40$).

For FBC the computation of $\rho_v(T)$ has been performed on two lattice sizes $L \times L$ and $2L \times 2L$ ($L = 30$), which was enough to draw some conclusions.

There is a shift in the mean value of the vortex pair-creation energy, which may be understood if typical equilibrium spin configurations at temperatures near T_c are considered. In figure 8, for a 30×30 spin lattice and the PR model with FBC, representative equilibrium configurations of vortices for four temperatures around T_c are shown. Free vortices as well as vortex–antivortex pairs tend to appear near the system boundaries. It should be noted that for FBC the restriction $\Sigma_i m_i = 0$ is not fulfilled and isolated vortices may appear.

Holz and Gong (1987) have analysed the PR model in a square lattice defined for a semi-infinite plane ($y \geqslant 0$). The vortices interaction Hamiltonian is given by

$$H_v = 2\pi J\left[\sum_{i=1}^{N} m_i^2(\ln(2y_i/a) + \tfrac{1}{2}\pi) - \sum_{i\neq j}^{N} m_i m_j \ln\left(\frac{(y_i - y_j)^2 + (x_i - x_j)^2}{(y_i + y_j)^2 + (x_i - x_j)^2}\right)^{1/2}\right] \qquad (16)$$

where the sums extend over the N vortices in the semi-plane and a is the lattice parameter. In this Hamiltonian the vortices interact with their vortex images, since FBC are equivalent to Von Neumann boundary conditions in the electrostatic analogy of the model (neutral Coulomb plasma). The single vortex energy is an increasing function of its distance to the boundary and therefore its creation near the edge is favoured. The same

happens with the vortex pairs, which are attracted to the boundary. The diffusion of a single vortex inside the bulk requires less energy than the dissociation of a vortex pair and due to this effect the transition is softened. The presence of single vortices on lattices with FBC decreases the correlations at the boundaries and, therefore, is responsible for the decrease of susceptibility at low temperatures with respect to the susceptibility for lattices with PBC.

It may be stated, by simple inspection of figure 8, that binding vortex–antivortex pairs as well as unbinding (isolated) vortices are present mainly at the boundaries and even below T_c. However, as the excellent fitting of ρ_v to the Arrhenius law makes clear, only one activation energy seems to be relevant in both cases. For PBC this energy must be related to vortex–antivortex pair creation (Tobochnik and Chester 1979). For FBC the situation is less clear. There are two possible activation processes: one is related to pair creation and another associated with the isolated vortex which always appears at the boundaries. However, the energy of an isolated vortex should not be much different from that of the pair (see equation 16), because the former is created along with its 'vortex image'. Moreover, since the pairs interact also with their images, their creation energy must decrease, which explains the differences of E_v between PBC and FBC.

The main conclusion to be drawn concerns the fundamental role that boundary conditions play when one deals with finite-size systems. For the 2D-planar models here described, not only quantitative but also qualitative differences are found. The boundary conditions modify the way in which the vortex pairs appear and break the SRO. Furthermore, single vortices are not forbidden at low temperatures, when FBC are chosen. Therefore, it is clear that any quantitative analysis of finite-size systems, such as clusters, cannot avoid the problem of the boundary conditions.

Acknowledgments

The authors sincerely acknowledge Professor D Gonzalez for his valuable comments on the manuscript. The financial support of the Spanish Comision Interministerial de Ciencia y Tecnología (CICYT- project PB86-0187) is also acknowledged.

References

Ami S and Kleinert H 1982 *Phys. Rev.* B **33** 4692
Barber M N 1983 *Phase Transition and Critical Phenomena* vol. 8 ed. C Domb and J L Lebowitz (New York: Academic)
Diep H T, Ghazali A and Lallemand P 1985 *J. Phys. C: Solid State Phys.* **18** 5881
Domb C and Green M S (ed.) 1974 *Phase Transition and Critical Phenomena* vol 3 (New York: Academic)
Dresselhaus M S (ed.) 1986 *Intercalation in Layered Materials* (New York: Plenum)
Falo F and Navarro R 1989 *J. Physique Coll.* **49** C8-1399
Ferer M and Velgakis M J 1983 *Phys. Rev.* B **27** 314
Ferer M, Aidinejad A H and Velgakis M J 1984 *J. Appl. Phys.* **55** 2438
Gerling R W and Landau D P 1984 *Springer Series in Solid State Physics* vol 54 (Berlin: Springer)
Holz A and Gong C 1987 *Phys. Lett.* A **120** 469
Janke W and Kleinert H 1986 *Nuclear Physics* B **270** 135
José J V, Kadanoff L P, Kirkpatrick S and Nelson D R 1977 *Phys. Rev.* B **16** 1217
Kawabata C and Bishop A R 1986 *Z. Phys.* B **65** 225
Kosterlitz J M 1974 *J. Phys. C: Solid State Phys.* **7** 1046
Kosterlitz J M and Thouless D J 1973 *J. Phys. C: Solid State Phys.* **6** 1181
Landau D P and Binder K 1981 *Phys. Rev.* B **24** 1391

Puértolas J A, Navarro R, Palacio F, Bartolomé J, González D and Carlin R L 1985 *Phys. Rev.* B **31** 516
Regnault L P, Rossat-Mignod J, Henry J Y, Pynn R and Petitgrand D 1984 *Springer Series in Solid State Physics* vol 54 (Berlin: Springer)
Samuel S 1982 *Phys. Rev.* B **25** 1755
Savit R 1980 *Phys. Rev.* B **22** 3443
Sinha S 1980 *Ordering in Two Dimensions* (Amsterdam: North-Holland)
Szeto K Y and Dresselhaus G 1985 *Phys. Rev.* B **32** 3142
Tobochnik J and Chester G V 1979 *Phys. Rev.* B **20** 3761